

Single-pulse MIG welded Perform 700 steel joints with various welding parameters

Fatih Özen^{1*}

¹Welding Programme Division, Department of Machine and Metals, Beşiri Industrial Organized Zone Vocational College, Batman University, 72100, Batman, Türkiye

Orcid: F. Özen (0000-0002-2915-8456)

Abstract: In this work, Perform 700 steel sheets with a 5-mm thickness were welded with a single-pulse MIG welding method with different welding currents and welding speeds. The welded specimens were subjected to tensile tests, hardness measurements, and microstructural observations. According to the results, the heat input played a significant role in the tensile strength of the joint. The maximum tensile strength was obtained as 594.75 MPa at 140A welding current and 450 mm/min welding speed. The tensile specimens consistently separated between the fusion zone and the heat-affected zone. The heat-affected zones have exhibited tempered martensitic structure. The tempering effect increased the sizes of the martensitic structure; therefore, the hardness was significantly increased. However, the fusion zone, which consisted of a bainitic structure inside the ferrite matrix, exhibited soft and ductile behavior. The boundary of the soft fusion zone and hard heat-affected zone formed the weakest point in the joint.

Keywords: welding, joining, mechanical properties, perform steel, S700MC, single-pulse, MIG weld

1. Introduction

Limited fossil fuels, the global warming effect induced by carbon emissions, and increasing the level of safety standards have caused a dramatic change in steel technology [1,2]. However, steel is abundant, easy to produce, rigid, and cheaper than non-ferrous metals, making it an inevitably useful material in various industries. The key motivation is to decrease the weight of a design by increasing its strength without compromising safety, allowing for flexible and light design structures [3]. Although developed steels are not cheaper than conventional steels, they offer lower consumption of the steels, decreasing both carbon emissions and material expenses [4].

With these motivations, numerous steel types have been developed. Among these steels, high-strength low alloy (HSLA) and advanced high-strength steel (AHSS) families have drawn attention in various industries including automotive, transportation, marine, and construction [5–8]. Especially, HSLA steels have been commonly employed in structural applications such as highway barriers, bridge cables, car frames, truck bodies, electrical transmission structures, street light posts, etc. [9].

PERFORM steels are an important member of HSLA steels, which is a trademark of ThyssenKrupp AG (Germany). Among the PERFORM steels, PERFORM 700, which

is also known as S700MC, is one of the most employed steel grades [10]. Due to its popularity, much work has been done on welding similar and dissimilar joints [11-20].

Petronis et al. [11] investigated the hybrid laser-arc weldability of S700MC joints with different thicknesses. They reported that although full penetration was obtained at a laser power of 6 kW, horizontal and vertical positions have exhibited poor weldability at high speeds of the weld. Silva et al. [12] studied MAG welding of S700MC with a low arc technique. It was found that usage of the blowtorch has decreased both the weld energy consumption and splinters while retaining the mechanical performance of the welded joint. Szymczak et al. [13] examined the effect of the welding operation on the mechanical performance of S700MC joints subjected to various types of tests. They noted that S700MC steel is sensitive to the heat input applied by the welding operation in terms of mechanical properties. Ferdinandov et al. [14] studied the mechanical performance of submerged arc-welded S700MC joints with various weld gaps. They reported a limited reduction in the yield strength since most of the plastic deformation is formed in both the heat-affected and fusion zones. Moravec et al. [15] studied the fatigue life performance of MAG-welded S700MC. They reported that the application of the double-sided fillets adversely influenced fatigue life. Tomków et al. [16] investigated the underwater welding of S700MC with rutile

* Corresponding author.
Email: fatih.ozen@batman.edu.tr



electrodes and described that the maximum hardness in the heat affected did not exceed the critical threshold. Eva et al. [17] simulated the welded S700MC joint by joule heating effect and carried out various mechanical tests. They pointed out that the transformations taking place in the heat-affected zone have a profound influence on the fracture response of the welded joint. Kik et al. [18,19] studied a numerical verification analysis of cyclic thermal application and the effect of annealing temperature on the residual stress level, respectively. They noted that S700MC is overly sensitive to the applied temperature in terms of both stress levels and phase transitions. Sebestova et al. [20] investigated the fatigue properties of hybrid laser-TIG welded S700MC and S460MC steels. They stated that the fatigue cracks frequently initiate from the interface between the fusion zone and the heat-affected zone.

The works regarding the Perform steels emphasize the sensitivity against the exposure of the heat application, especially in welding processes. Therefore, applying low-heat inputs in the welding of Perform steels is of foremost importance. In this study, investigating the single-pulse MIG welding technique in the welding of Perform 700 steels is of high importance. Although a great deal of studies have been conducted in these steel grades, single-pulse MIG welding has not been thoroughly investigated. The microstructural and mechanical properties are investigated using microstructural observation, hardness measurements, and tensile tests with various welding parameters.

2. Materials and Method

The Perform 700 steel sheets with 4-mm thickness were acquired by the local dealers. The sheets were sliced to 150x120-mm dimensions. The weld surfaces of the specimens were cleaned with acetone to remove oil and dirt. Figure 1 shows the welding tractor manipulator and welding setup for the experiments. The welding tractor manipulator was employed to attain sound and reliable weld joints. The tractor manipulator was also used to adjust the welding speeds.

A Magmaweld IDS 320MM Pulse welding machine was employed in the experiments. The shielding gas consisted of 86% Ar, 12% CO₂, and 2% O. SG-2 weld wire was employed in the experiments. The chemical compositions of the Perform 700 steel and SG-2 wire are presented in Table 1. Standard arc distance was kept between weld filler wire and BM.

Table 2 illustrates the welding experiment design for single-pulse MAG welding. Two main motivations were planned. First, hold the welding speed while increasing the current intensity, second, stabilizing the current intensity while increasing the welding speed. To obtain this goal, welding speeds were kept constant in the first three experiments while welding currents were fixed in experiment numbers 4, 5, and 6. The welded specimen was sliced with a 25-mm width. Three of them were used for tensile tests, and the last specimen was employed in hardness and microstructural observations. The weld start and end distances with 25 mm were thrown to obtain sound welds,

Table 1. Chemical compositions of the Perform 700 and SG-2 filler metal wire.

Material	Elements (wt.%)											
	C	Mn	Si	Mo	Ni	P	S	Al	Ti	Nb	V	Fe
Perform 700	0.047	1.966	0.205	0.156	0.161	0.005	0.006	0.034	0.058	0.066	0.061	Rest
SG-2 wire	0.075	1.516	0.851	-	-	-	-	-	-	-	-	Rest

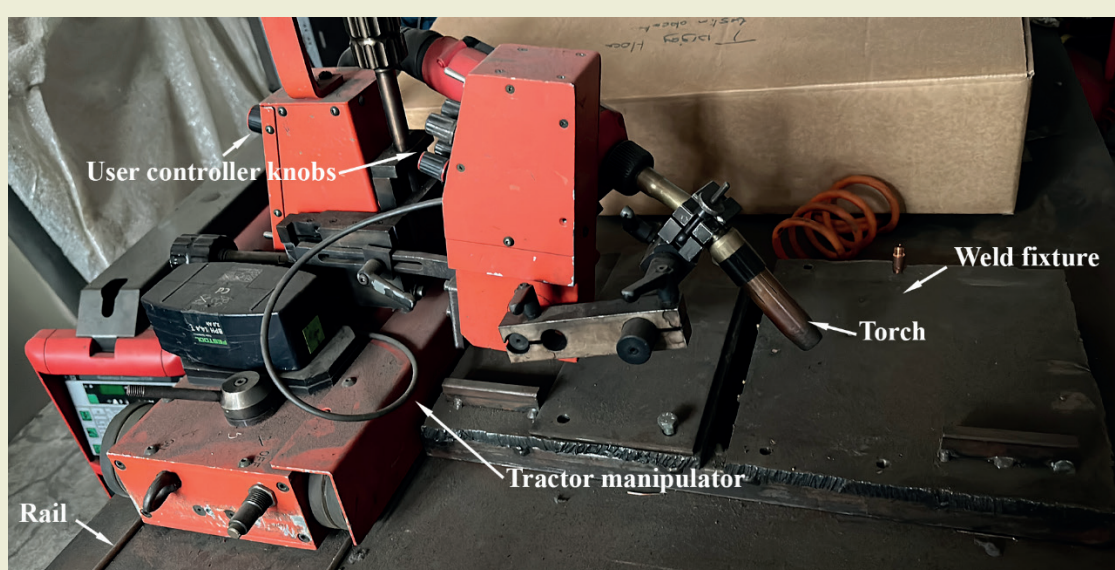


Figure 1. Welding setup for experiments

ensuring consistent welding parameters.

Table 2. Applied welding parameters for the experiments.

Experiment no.	Current (A)	Voltage (V)	Welding speed (mm/min)	Gas flow rate (l)
1	120	16.2	350	10
2	140	17.5	350	
3	160	19.3	350	
4	140	17.8	300	
5	140	17.8	400	
6	140	17.8	450	

Tensile tests were carried out with a universal testing device. Tensile speed was 10 mm/min. The average results were employed in the graphs. For the metallographic examination, conventional specimen preparation techniques were adopted. The final pass of polishing was executed with 1 μm Alumina suspension. The polished surfaces were etched with 4% Nital solution. The microstructures were examined by a Nikon L150A light microscope. Wilson hardness tester with Vickers indentation was used for line hardness measurements.

3. Results and Discussion

Since heat input is of high importance, the welding speeds and welding current were carefully designed. The heat input can be calculated using (1) [21]. Here, H is the heat input (kJ/mm), η is efficiency, I is the current density (A), E is the applied voltage (V) and S is the welding speed (mm/min).

$$H = \frac{I \cdot V \cdot 60}{S \cdot 1000} \eta \quad (1)$$

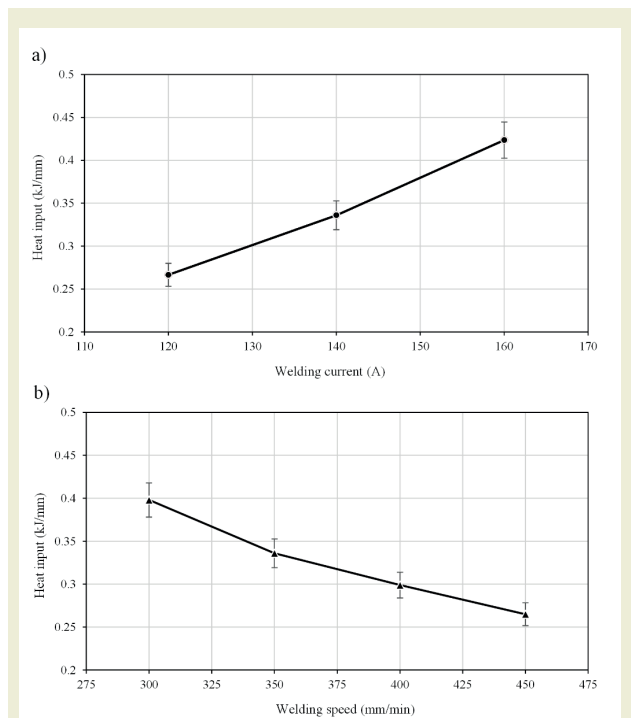


Figure 2. Calculated heat input in terms of a) various welding currents under a constant welding speed of 300 mm/min, and b) different welding speeds under a constant welding current of 140A

Figures 2a and 2. b illustrate calculated heat inputs both under a constant welding speed of 300 mm/min and under a constant welding current of 140A, respectively. As the applied welding current is increased, the heat input increases. The welding speed has opposite characteristics, the heat input decreases as the welding speed increases. This can be attributed to the accumulation of the applied heat during welding.

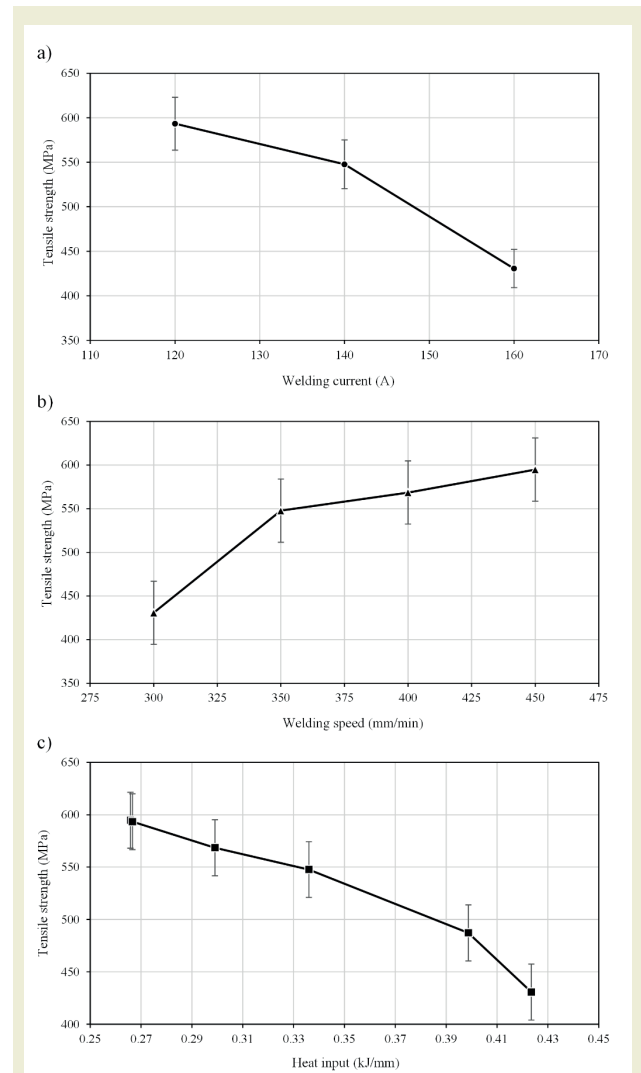


Figure 3. Tensile strength of the MIG welded joint in terms of a) Welding current, b) Welding speed, and c) Heat input.

The effect of welding current, welding velocity, and heat input on tensile strength of the single-pulse MIG welded Perform 700 joint is presented in Figure 3. a-c, respectively. The welding current and the welding velocity exhibit an inverse characteristic. This significant variation can be attributed to the heat input during welding. Elevated welding currents increase the heat input at the weld joint, and a slowdown in welding speed causes the accumulation of heat as well. The lowest tensile strength was obtained at a high welding speed and the maximum welding current, which is measured as 300 mm/min welding speed and 160A welding current, respectively. The maximum tensile strength was measured as 594.75 MPa at 140A welding current and 450mm/min welding speed.

Figure 4a-f shows the microstructure of single-pulse MIG welded joints with various magnifications. The weld microstructure can be divided into three sections: base metal (BM), heat-affected zone (HAZ), and fusion zone (FZ). The BM of the joint consists mostly of bainite and ferrite islands, with small fractions of martensite as well. Figure 5 shows line hardness measurements of the single-pulse MIG-welded joint. The BM of the Perform 700 exhibited an average hardness of 285 ± 5 Hv10. Then, the hardness increased in the HAZ, reaching the peak point, measured as 381 Hv10. As seen in Figure 4. e, the bainite transformed into tempered martensite. The grain sizes also increased in the HAZ. The hardness variation in the

HAZ does not have linear consistency. These hardness differences are attributed to coarse polygonal ferrites [22]. However, high hardness is yielded near the FZ/HAZ junction. Although the ferrite grains are softer than tempered martensite, the ferrite grains are not bigger than Vickers indentation, thereby measuring indentation has always touched not only ferrites but also the tempered martensite [16].

The hardness line from HAZ to FZ suddenly decreases. Although the hardness increased to a limited extent near the HAZ/FZ interface, the hardness decreased to 283 ± 5 Hv10, similar to that of BM. The hardness at the center-

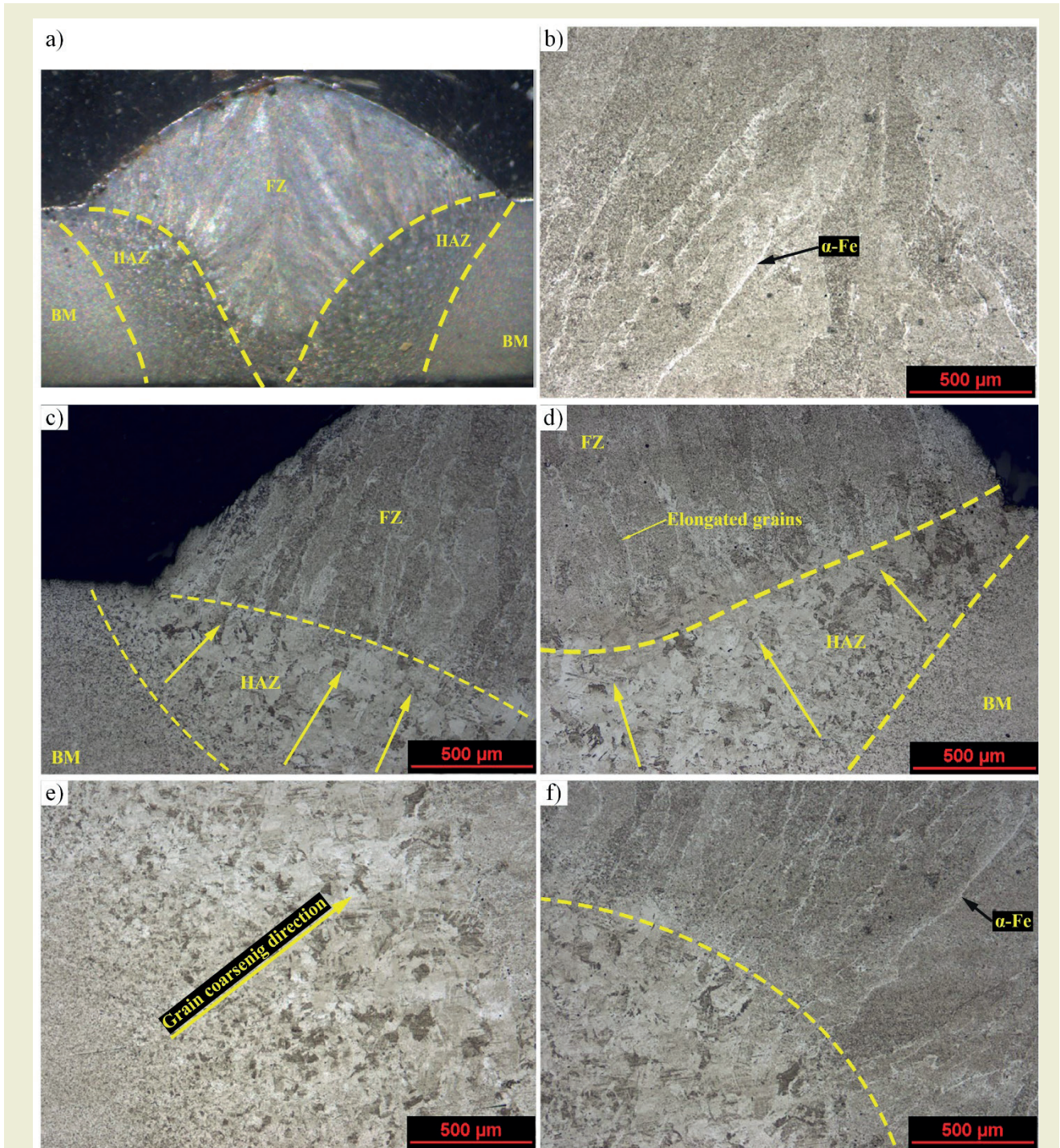


Figure 4. Micrographs of single-pulse MIG welded joints from different regions from; a) the whole joint macro image, b) FZ, c) Weld joint from left side, d) Weld joint from right side, e) HAZ, and f) HAZ/FZ interface

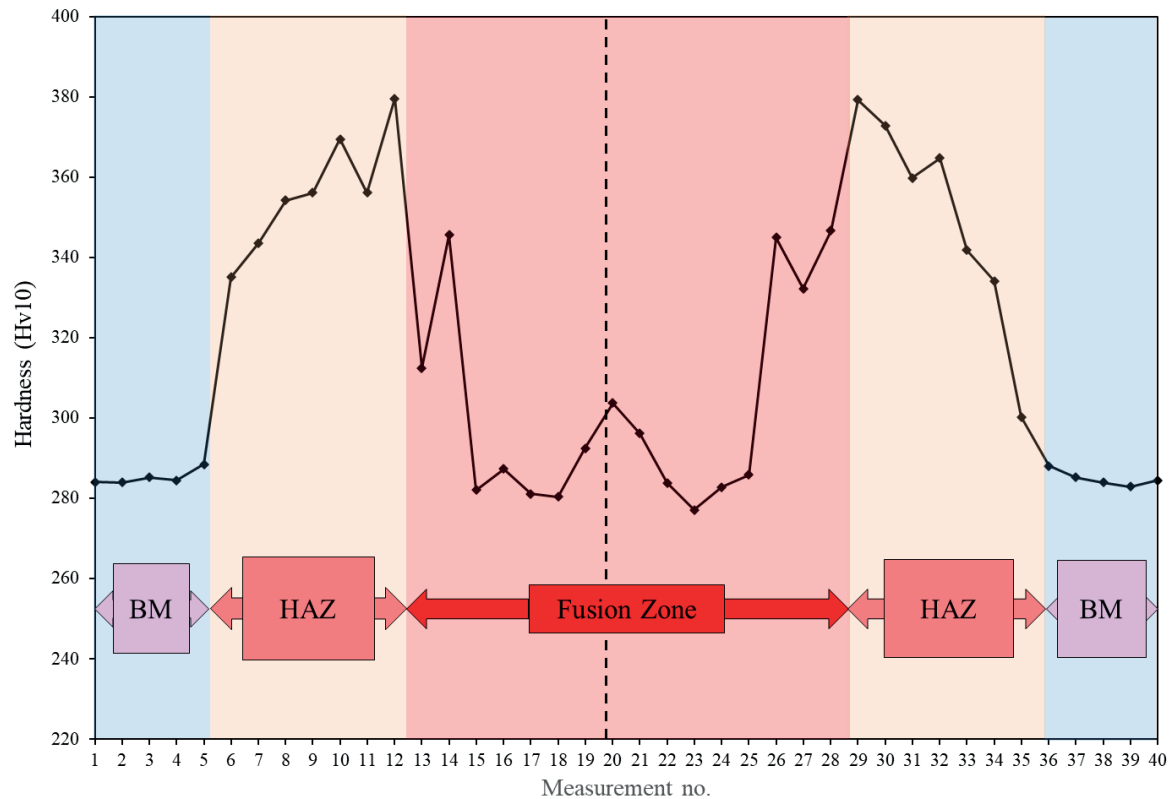


Figure 5. Line hardness measurement of the single-pulse MIG welded joint.

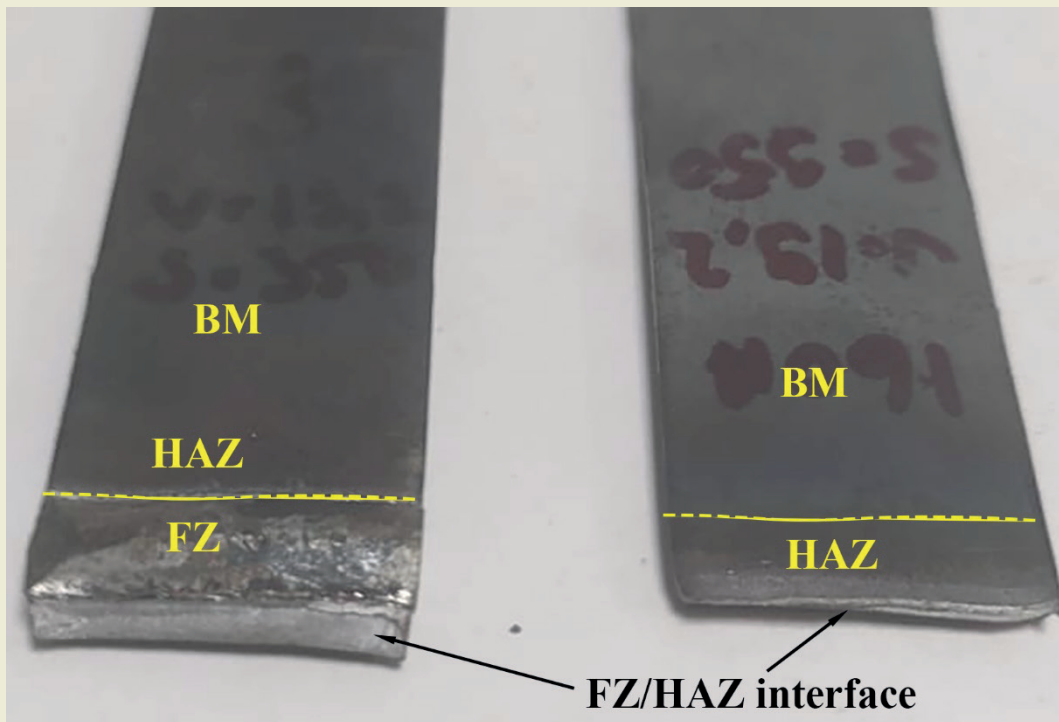


Figure 6. Rupture surface of single-pulse MIG welded tensile specimen.

line of the FZ increased to 306 Hv10 due to the orientation of the grains. The grains formed in the FZ have followed the cooling path and formed a neutral axis in the middle of the FZ. The grains have joined through the neutral centerline.

The FZ consists of mostly bainitic and ferritic grains. The

boundary of the grains is enveloped by α -ferrite as seen in Figure 4b. The bainitic formations are scattered through the α -ferrite matrix. Near the HAZ in FZ, the grains are refined, marking the boundary of the FZ. These refined grains increased the hardness at this location. Then, the hardness decreased in the FZ and exhibited a ductile structure due to scattered bainitic formations in the

ferrite matrix.

Figure 6 illustrates the rupture surface of a single-pulse MIG welded tensile specimen. The tensile specimens consistently separate from the FZ/HAZ interface. In other words, the FZ/HAZ interface represents the weakest point in the welded joint. This failure can be evaluated in terms of two factors. First, a significant hardness difference between the FZ/HAZ interface, creating a natural boundary between ductile and brittle structures. Second, the solidified grains follow the cooling direction, and the boundaries of the grains, surrounded by a soft α -ferrite, form a pathway for separation. Consequently, the entire welded tensile specimens become detached from the FZ/HAZ interface.

References

- [1] Park, G.W., Park, M., Kim, B.J., Shin, S., Kim, H.C., Park, I.W., et al. (2022). Microstructure and mechanical properties of a gas-tungsten-arc-welded Fe-24Mn-3.5Cr-0.4C high manganese steel pipe using a Fe-22Mn-2.34Ni-0.38C welding wire. *Materials Characterization*. 194(11): 1–12. doi: 10.1016/j.matchar.2022.112469.
- [2] Onar, V., (2022). Mechanical and Microstructural Characterizations of Resistance Spot Welded Dissimilar TWIP/304L Stainless Steel. *Transactions of the Indian Institute of Metals*. 75: 1731–1739. doi: 10.1007/s12666-021-02446-9.
- [3] Kekik, M., Özen, F., Onar, V., Aslanlar, S., (2022). Investigation effect of resistance spot welding parameters on dissimilar DP-1000HF/CP800 steel joints. *Sadhana - Academy Proceedings in Engineering Sciences*. 47(4): 1–17. doi: 10.1007/s12046-022-01977-1.
- [4] Bjorhovde, R., (2004). Development and use of high-performance steel. *Journal of Constructional Steel Research*. 60(3–5): 393–400. doi: 10.1016/S0143-974X(03)00118-4.
- [5] Özsaraç, U., Onar, V., Özen, F., Aslanlar, Y.S., Akkaş, N., (2019). Effect of current and welding time on tensile-peel strength of resistance spot welded TWIP 1000 and martensitic steels. *Indian Journal of Chemical Technology*. 26(4): 248–51.
- [6] Özsaraç, U., Onar, V., Özen, F., Aslanlar, Y.S., Akkaş, N., (2019). Effect of welding time on tensile-shear load in resistance spot welded TRIP 800 and microalloyed steels. *Indian Journal of Chemical Technology*. 26(4): 355–7.
- [7] Lun, N., Saha, D.C., Macwan, A., Pan, H., Wang, L., Goodwin, F., et al., (2017). Microstructure and mechanical properties of fiber laser welded medium manganese TRIP steel. *Materials and Design*. 131: 450–9. doi: 10.1016/j.matdes.2017.06.037.
- [8] Hong, S.-H., Eo, D.-R., Lee, S., Cho, J.-W., Kim, S.-J., (2023). Strong resistance to Zn-assisted liquid metal embrittlement of austenitic-TWIP/martensitic-HSLA multi-layered steel sheets additively manufactured by laser cladding. *Acta Materialia*. 258(March): 119224. doi: 10.1016/j.actamat.2023.119224.
- [9] Shreyas, P., Panda, B., Vishwanatha, A.D., (2021). Embrittlement of hot-dip galvanized steel: A review. *AIP Conference Proceedings*, vol. 2317. p. 1–15.
- [10] Phung, T.A., (2022). Experimental study on mechanical properties and microstructure of PERFORM 700 steel butt-welding joints using in high load-bearing structures. *Journal of Science and Technique*. 17(1): 53–63. doi: 10.56651/lqdtu.jst.v17.n01.301.
- [11] Petronis, E., Cerwenka, G., Emmelmann, C., (2017). Hybrid laser-arc welding of steel S700MC butt joints under different sheet thickness.
- [12] Silva, A., Szczucka-Lasota, B., Węgrzyn, T., Jurek, A., (2019). MAG welding of S700MC steel used in transport means with the operation of low arc welding method. *Welding Technology Review*. 91(3): 23–8. doi: 10.26628/wtr.v91i3.1043.
- [13] Szymczak, T., Makowska, K., Kowalewski, Z.L., (2020). Influence of the welding process on the mechanical characteristics and fracture of the s700mc high strength steel under various types of loading. *Materials*. 13(22): 1–17. doi: 10.3390/ma13225249.
- [14] Ferdinandov, N., Gospodinov, D., Ilieva, M., Radev, R., (2021). Influence of Weld Joint Preparation on the Mechanical Properties of High Strength Steel S700Mc Weldments. *METAL 2021 - 30th Anniversary International Conference on Metallurgy and Materials, Conference Proceedings*: 441–6. doi: 10.37904/metal.2021.4149.
- [15] Moravec, J., Sobotka, J., Novakova, I., Bukovska, S., (2021). Assessment the partial welding influences on fatigue life of s700mc steel fillet welds. *Metals*. 11(2): 1–16. doi: 10.3390/met11020334.
- [16] Tomków, J., Świerczyńska, A., Landowski, M., Wolski, A., Rogalski, G., (2021). Bead-on-Plate Underwater Wet Welding on S700MC Steel. *Advances in Science and Technology Research Journal*. 15(3): 288–96. doi: 10.12913/22998624/140223.
- [17] Schmidová, E., Bozkurt, F., Culek, B., Kumar, S., Kuchariková, L., Uhrčík, M., (2019). Influence of Welding on Dynamic Fracture Toughness of Strenx 700MC Steel. *Metals*. 9(5): 494. doi: 10.3390/met9050494.
- [18] Kik, T., Górka, J., Kotarska, A., Poloczec, T., (2020). Numerical Verification of Tests on the Influence of the Imposed Thermal Cycles on the Structure and Properties of the S700MC Heat-Affected Zone. *Metals*. 10(7): 974. doi: 10.3390/met10070974.
- [19] Kik, T., Moravec, J., Švec, M., (2020). Experiments and Numerical Simulations of the Annealing Temperature Influence on the Residual Stresses Level in S700MC Steel Welded Elements. *Materials*. 13(22): 5289. doi: 10.3390/ma13225289.
- [20] Šebestová, H., Horník, P., Mrňa, L., Jambor, M., Horník, V., Pokorný, P., et al., (2020). Fatigue properties of laser and hybrid laser-TIG welds of thermo-mechanically rolled steels. *Materials Science and Engineering: A*. 772(December 2019): 138780. doi: 10.1016/j.msea.2019.138780.
- [21] ONAR, V., (2020). Robotik MAG Kaynak Metodunda XAR 500 Serisi Çeliklerin Mikrosertliğine Farklı Kaynak Akımlarının ve

4. Conclusions

The Perform 700 steel sheets were successfully welded using single-pulse MIG method with SG-2 wire. The heat input has played a crucial role in determining the tensile strength. The main affecting factor is the degree of the heat input. The heat input degraded the bainitic BM into tempered martensite. The FZ/HAZ interface functioned as a boundary between hard highly tempered martensite and soft granular bainitic within the ferritic matrix. As a result, this natural boundary compromised the weakest point for the single-pulse welded joint. The locations of ruptures on the separation surfaces also confirm this weakness. The abrupt decrease in hardness from HAZ to FZ contributed to FZ/HAZ separations.

Hızlarının Etkisi. Düzce Üniversitesi Bilim ve Teknoloji Dergisi.
8(1): 1193–203. doi: 10.29130/dubited.646727.
[22] Fayazi Khanigi, A., Farnia, A., Ardestani, M., Torkamany, M.J.,
(2020). Microstructure and mechanical properties of low power

pulsed Nd:YAG laser welded S700MC steel. Sadhana - Academy
Proceedings in Engineering Sciences. 45(1): 1–13. doi: 10.1007/
s12046-020-1279-6.